Biophysical Journal
Article

Biophysical Society

Regulation of Active ICAM-4 on Normal and Sickle Cell Disease RBCs via AKAPs Is Revealed by AFM

Jing Zhang,[1] Krithika Abiraman,[2] Sasia-Marie Jones,[3] George Lykotrafitis,[1,2,*] and Biree Andemariam[3,*]
[1]Department of Mechanical Engineering and [2]Department of Biomedical Engineering, University of Connecticut, Storrs, Connecticut; and [3]New England Sickle Cell Institute, Division of Hematology-Oncology, Neag Comprehensive Cancer Center, UCONN Health, University of Connecticut, Farmington, Connecticut

ABSTRACT Human healthy (wild-type (WT)) and homozygous sickle (SS) red blood cells (RBCs) express a large number of surface receptors that mediate cell adhesion between RBCs, and between RBCs and white blood cells, platelets, and the endothelium. In sickle cell disease (SCD), abnormal adhesion of RBCs to endothelial cells is mediated by the intercellular adhesion molecule-4 (ICAM-4), which appears on the RBC membrane and binds to the endothelial $\alpha v\beta 3$ integrin. This is a key factor in the initiation of vaso-occlusive episodes, the hallmark of SCD. A better understanding of the mechanisms that control RBC adhesion to endothelium may lead to novel approaches to both prevention and treatment of vaso-occlusive episodes in SCD. One important mechanism of ICAM-4 activation occurs via the cyclic adenosine monophosphate-protein kinase A (cAMP-PKA)-dependent signaling pathway. Here, we employed an in vitro technique called single-molecule force spectroscopy to study the effect of modulation of the cAMP-PKA-dependent pathway on ICAM-4 receptor activation. We quantified the frequency of active ICAM-4 receptors on WT-RBC and SS-RBC membranes, as well as the median unbinding force between ICAM-4 and $\alpha v\beta 3$. We showed that the collective frequency of unbinding events in WT-RBCs is not significantly different from that of SS-RBCs. This result was confirmed by confocal microscopy experiments. In addition, we showed that incubation of normal RBCs and SS-RBCs with epinephrine, a catecholamine that binds to the β-adrenergic receptor and activates the cAMP-PKA-dependent pathway, caused a significant increase in the frequency of active ICAM-4 receptors in both normal RBCs and SS-RBCs. However, the unbinding force between ICAM-4 and the corresponding ligand $\alpha v\beta 3$ remained the same. Furthermore, we demonstrated that forskolin, an adenylyl cyclase activator, significantly increased the frequency of ICAM-4 receptors in WT-RBCs and SS-RBCs, confirming that the activation of ICAM-4 is regulated by the cAMP-PKA pathway. Finally, we showed that A-kinase anchoring proteins play an essential role in ICAM-4 activation.

INTRODUCTION

Sickle cell disease (SCD) is a blood disorder that results from a recessively inherited point mutation occurring in the β-globin gene. This gives rise to abnormal (sickle) hemoglobin (HbS), which in deoxygenated conditions polymerizes to form stiff filaments (1–3), causing a distortion in the shape of the red blood cells (RBCs) from biconcave to sickled. Because of their distorted shape, RBCs carrying the defective hemoglobin HbS are called sickle RBCs (SS-RBCs). In addition to their irregular shape, compared with normal (wild-type (WT)) RBCs, SS-RBCs are stiffer and more viscous, and show higher adhesion to other RBCs, platelets, leukocytes, and the endothelium (2,4–8). Abnormal SS-RBC adhesion leads to delayed microvascular passage of deoxygenated RBCs, inducing sickling and entrapment of RBCs, a key trigger of vaso-occlusive episodes (VOEs), which are the hallmark of SCD (9). In addition, the degree of RBC adhesion has been shown to correlate with the clinical severity of VOEs (6,10).

Previous studies by our group and others (9,11,12) demonstrated that increased SS-RBC adhesion is due to enhanced expression of functional adhesion receptors on the RBC membrane. RBC receptor activation is dependent upon intracellular signaling pathways (5) that can be activated by extracellular stimuli. One such pathway is cAMP-PKA, which can be activated by epinephrine, a catecholamine that binds to G protein-coupled receptor (9,12,13). It has been shown that the cAMP-PKA pathway directly regulates the activation of basal cell adhesion molecule/Lutheran (BCAM/Lu) on the RBC surface (7,12,14). These BCAM/Lu receptors in turn bind to laminin-α-5, a component of the endothelial subcellular matrix (14). In addition, studies using a variety of adhesion assays, including micropipetting and perfusion chambers, revealed

Submitted July 15, 2016, and accepted for publication November 28, 2016.
*Correspondence: gelyko@engr.uconn.edu or andemariam@uchc.edu
Editor: David Piston
http://dx.doi.org/10.1016/j.bpj.2016.11.3204

that SS-RBCs adhere to endothelial cells (10,15), inducing endothelial injury and inflammation, and likely contributing to VOEs (6,10,16–18). Zennadi et al. (7) further showed that intercellular adhesion molecule-4 (ICAM-4) is the primary receptor that mediates the adhesion of SS-RBCs to endothelial cells, and that the ligand for the ICAM-4 receptor is the endothelial $\alpha v\beta 3$ integrin (7,19,20). They also reported that epinephrine can stimulate the activation of ICAM-4 at least partially via the cAMP-PKA-dependent signaling pathway. Specifically, epinephrine stimulates RBC $\beta 2$-adrenergic receptors ($\beta 2$-ARs) through activation of the α subunit of the associated G protein ($G\alpha s$) by exchanging its bound guanosine diphosphate (GDP) to guanosine triphosphate (GTP) (21,22). The activated $G\alpha s$, together with GTP, then dissociates from the β and γ subunits to further stimulate adenylyl cyclase (AC) (23,24). AC catalyzes the conversion of adenosine triphosphate (ATP) to cAMP, which then activates PKA (12,25). PKA in turn phosphorylates ICAM-4. The cAMP-PKA pathway is described in Supporting Materials and Methods in the Supporting Material (Fig. S1).

Our group first demonstrated that scaffold proteins termed A-kinase anchoring proteins (AKAPs) are critical for mediating the adherence of RBC BCAM/Lu receptors to laminin (12). The AKAP family includes ~50 structurally diverse but functionally similar scaffolding proteins that contain 1) a common PKA-anchoring domain that binds to the regulatory subunit of PKA (26–28) and 2) a unique subcellular targeting domain that guides the PKA-AKAP complex (21,29,30). AKAPs anchor PKA to specific subcellular sites, thereby guiding PKA activity toward specific locations in the cell, such as the plasma membrane (31), where PKA can alter the phosphorylation state of neighboring RBC receptors (26). It has been postulated that AKAPs mediate cAMP-PKA-dependent activation of RBC adhesion receptors via this mechanism (12).

In this study, we extended our work to investigate the effects of cAMP-PKA pathway manipulation on 1) the binding between ICAM-4 and $\alpha v\beta 3$, and 2) the expression of active ICAM-4 receptors on the membrane of both WT-RBCs and SS-RBCs. We also investigated whether AKAPs play a role in ICAM-4 activation. We implemented single-molecule force spectroscopy (SMFS) by using an atomic force microscope (AFM), which allows for the detection of single functional receptors on cells as well as measurements of the unbinding force between a receptor and the corresponding ligand (12,32–38). It also allows detection of variations in the collective frequency (CF) of active ICAM-4 receptors on the RBC membrane. We used several biochemical reagents that manipulate the cAMP-PKA pathway and the AKAP-PKA complex to regulate ICAM-4 activation. In addition, we used confocal microscopy to corroborate our AFM results.

Our experiments confirmed, at the single-molecule level, that activation of the ICAM-4 receptors depends upon the cAMP-PKA pathway. Using both SMFS and confocal microscopy, we found that the surface expression of active ICAM-4 receptors did not differ significantly between WT-RBCs and SS-RBCs. We also showed that epinephrine increased the expression of active ICAM-4 receptors in RBC samples from both healthy donors and SCD patients. Importantly, we demonstrated that this activation is mediated by AKAPs. In addition, we found that although the CF of active ICAM-4 receptors was modulated via the cAMP-PKA pathway, the mean value of the unbinding force between active ICAM-4 and $\alpha v\beta 3$ did not change even at higher surface expressions of active ICAM-4. This means that activation of ICAM-4 did not alter the unbinding force and that nanoclusters of ICAM-4 receptors were not formed in detectable numbers. This result, along with the finding that epinephrine activates ICAM-4 in both WT- and SS-RBCs, contrasts with results based on flow-chamber assays that showed that epinephrine did not significantly increase ICAM-4-dependent adhesion on WT-RBCs. The findings of this work might be of clinical importance in the context of drug development for the prevention and treatment of VOEs in SCD because they suggest that enhanced adhesion events between RBCs and the endothelium can be hindered by the introduction of biomedical reagents that act not only along the cAMP-PKA pathway but also on the AKAP-PKA complex.

MATERIALS AND METHODS

Human subjects and blood preparation

Our clinical protocol was approved by the institutional review boards of the University of Connecticut-Storrs and UCONN Health. For inclusion in the study, healthy volunteers had to be at least 7 years old and have a normal hemoglobin electrophoresis. Healthy volunteers were excluded from the study if they were pregnant, breastfeeding, or within 3 months postpartum; had received antilipid therapy within the previous week; were taking an investigational drug; or had received a blood transfusion within the previous 3 months. Inclusion/exclusion criteria for homozygous SCD (SS) patients: SCD patients were included in the study if they had documented homozygous SS disease, were at least 7 years old, and were in steady state. Steady state was defined as not having received a parenteral opioid in the previous 4 weeks, had pain no greater than the usual daily level for 4 weeks, and had no increase in their usual nonparenteral opioid medication in the previous 4 weeks. SCD patients were excluded from the study if they were pregnant, breastfeeding, or within 3 months postpartum; had received antilipid therapy within the previous week; were taking an investigational drug; had been treated with hydroxyurea (HU); or had received a blood transfusion within the previous 3 months. HU treatment was an exclusion criterion because HU has been shown to affect RBC adhesion to laminin by inhibiting phosphorylation of BCAM/Lu (12,39), and we reasoned that HU might act in a similar way to inhibit activation of ICAM-4. None of the SCD subjects had chronic organ damage. The demographic and clinical characteristics of the subjects are provided in Table 1.

Blood samples were obtained from freshly drawn, heparin-anticoagulated venous blood from eligible volunteers after they provided informed consent. Whole blood was centrifuged at $145 \times g$ for 5 min at 4°C to separate the RBCs. The plasma and buffy coat were extracted and discarded. Then, the remaining RBCs were washed three times with Alsever's solution and stored at 4°C for up to 7 days. We note that the experiments were performed in normal, nonhypoxic conditions. This is because hypoxia (6) and

TABLE 1 Demographic and Clinical Characteristics of the Blood Donors

SCD Patient		Healthy Volunteer	
	$n = 4$		$n = 3$
Age, mean, SD	26 (5)	Age, mean, SD	40 (3)
Gender, *n*, %		Gender, *n*, %	
male	4 (100)	female	3 (100)
Race, *n*, %		Race, *n*, %	
African-American	4 (100)	African-American	2 (67)
Genotype, *n*, %		White	1 (33)
HbSS	4 (100)		
Hemoglobin, g/dL,		Genotype, *n*, %	
mean, SD	9 (0)	HbAA	3 (100)
Leukocyte count,			
K/μL, mean, SD	14 (2)		
Platelet, K/μL,		Hemoglobin, g/dL,	
mean, SD	502 (181)	mean, SD	13 (1)
Neutrophil, %,		Leukocyte count, K/μL,	
mean, SD	53 (15)	mean, SD	6 (2)
Reticulocytes, %,		Platelet, K/μL, mean, SD	284 (64)
mean, SD	13 (5)		
LDH, U/L, mean, SD	444 (66)	Neutrophil, %, mean, SD	57 (10)

the consequent changes in the viscoelastic properties of SS-RBCs (40) may play a role in the variation of RBC adhesion, adding another parameter to the main focus of this work, which is the cAMP-PKA pathway. We also note that in SS patients the reticulocyte count average was 13% ± 5% (see Table 1), which is increased compared with healthy donors whose reticulocyte count is typically close to 0.5–2% (41). In our experiments, we chose to test only RBCs that had the characteristic biconcave shape to exclude reticulocytes, which typically had irregular shapes in our samples (see Supporting Materials and Methods and Fig. S2).

Ligand and reagents

Human integrin $\alpha v\beta 3$ protein (100 μg/mL, diluted with PBS) was obtained from Millipore (Billerica, MA). Alsever's solution, epinephrine (16.39 nM, reconstituted in Alsever's solution), forskolin (FSK; 0.49 μM, reconstituted in DMSO), and bovine serum albumin (BSA; 100 μg/mL, reconstituted in PBS) were purchased from Sigma-Aldrich (St. Louis, MO). St-Ht31 inhibitor peptide and St-Ht31P control peptide (both 81.97 nM, reconstituted in Alsever's solution) were purchased from Promega (Madison, WI). RBCs were treated with the above reagents at 37° for 30 min unless otherwise indicated.

AFM cantilever probe functionalization

Soft silicon nitride cantilevers with silicon nitride tips were purchased from Bruker Nano (Camarillo, CA). The tip height was between 2.5 and 8 μm and the nominal tip radius was 20 nm. The nominal spring constant of the applied cantilever was 30 pN/nm. The actual spring constant under the experimental condition (in Alsever's solution at 37°C) was calculated via a thermal-noise-based method (42,43).

Glutaraldehyde functionalization

Silicon nitride probes (Bruker AFM Probes, Camarillo, CA) were first amino-functionalized with 2% v/v 3-aminopropyltriethoxysilane in acetone (Sigma-Aldrich) for 10 min and then rinsed with deionized (DI) water. The probes were soaked in 0.5% v/v glutaraldehyde (solution in DI water) for 30 min, rinsed again with DI water, and incubated in a 100 μg/mL $\alpha v\beta 3$ solution. After 30 min, the probes were rinsed with DI water and immersed in 100 μg/mL of BSA for 1 min to block the remaining aldehyde groups. The probes were stored in PBS at 4°C and used within 3 days.

Acetal-PEG-NHS-$\alpha v\beta 3$ functionalization

Silicon nitride probes were functionalized with $\alpha v\beta 3$ via acetal-PEG-NHS (Institute of Biophysics, Johannes Kepler University, Linz, Austria) according to the manufacturer's instructions (http://www.jku.at/biophysics/content).

AFM setup and data recording

Experiments were performed using an MFP-3D-BIO AFM (Asylum Research, Santa Barbara, CA) that was mounted on an inverted microscope (Axiovert A1, Zeiss, Oberkochen, Germany). Using the microscope, we were able to position the AFM cantilever on a chosen RBC (Fig. 1 *A*) that was <10 μm in diameter and possessed an explicit circular biconcave shape indicative of RBC maturity and functionality. RBCs were pretreated with specific biomedical reagents and incubated at 37°C (30 min for epinephrine and FSK; 2 h for St-Ht31 and St-Ht31P). For each reagent, five RBCs from each subject were tested. RBCs were seeded in a glass-bottom petri dish (Ted Pella, Redding, CA) that was pretreated with 1 mg/mL poly-L-lysine solution (Sigma-Aldrich) for 15 min at room temperature. Under these conditions, RBCs adhered slightly to the substrate while they maintained their biconcave shape. During the cantilever retraction, RBCs were not pulled off the substrate, as we could clearly determine via the inverted microscope.

Adhesive interactions were quantified by recording force-distance curves at 32×32 points, distributed in a 1 μm^2 area of the RBC membrane, between an $\alpha v\beta 3$-functionalized cantilever and ICAM-4 receptors expressed on the RBC membrane. Each curve recorded a complete approach and retraction cycle. We have shown that measurements at 1024 points uniformly distributed in a 1 μm^2 area give a representative result for a specific tested RBC.

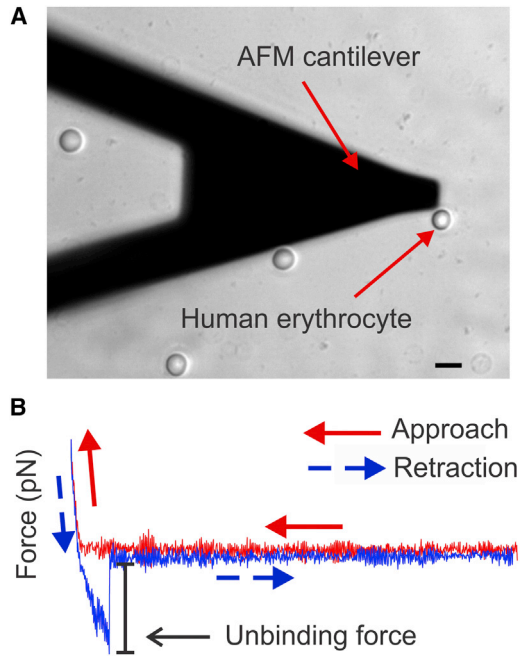

FIGURE 1 SMFS. (*A*) Optical microscopy image showing the shadow of an AFM cantilever and a representative human RBC. The scale bar corresponds to 10 μm. (*B*) Force curve plot exhibiting an unbinding event. The red curve represents the approach of the cantilever to the RBC surface membrane and the blue curve represents retraction of the cantilever from the RBC. The sharp change in the magnitude of the retraction force signifies the unbinding force. To see this figure in color, go online.

We note that because AFM experiments (and the subsequent data processing) are time consuming and often detrimental to tested cells, we have standardized the optimum scanning area for SMFS experiments on RBCs to be 1 μm^2 (44). We processed the AFM data using our in-house-developed code, named FRAME (Force Review Automation Environment) (45). An unbinding force was determined as the magnitude of the abrupt drop to zero on the retraction force-displacement curve with a rupture event (Fig. 1 *B*). The approach and retraction speed was 800 nm/s, which gave a nominal loading rate of 24,000 pN/s. At this speed, the unbinding measurements were not significantly affected by hydrodynamic forces (46). A specific trigger point/threshold was set to control the indentation depth and to ensure that the same nominal maximum force was applied to each RBC. The corresponding probe travel distance was ~200 nm, which meant the probe was in contact with the RBC membrane for ~1/4 s before retraction. We only considered the interactions for which the effective spring constants (k_{eff}) were <10 pN/nm, which in combination with the retraction speed ensures that the influence of k_{eff} is not significant for SMFS experiments (47). The effective spring constants were obtained from the slopes of the curves adjacent to the unbinding-force drops (48,49). The unbinding forces were plotted as a force map displaying the spatial distribution of the active ICAM-4 receptors on the RBC surface (Fig. 2 *A*). The color of each spot represents the value of the unbinding force obtained from the corresponding retraction path. CF% is defined as the percentage of all unbinding events divided by the total number of measurements, which is $32 \times 32 = 1024$ for each cell multiplied by the number of tested cells for each subject's blood sample. The CF represents the population of active ICAM-4 receptors that are capable of binding to $\alpha v\beta 3$. This approach allowed us to observe changes in the force maps due to modulation of the CF of activated ICAM-4 receptors in the presence of biochemical reagents that interfere with the cAMP-PKA pathway and the AKAP-PKA complex.

Specificity of the binding of $\alpha v\beta 3$ ligands to ICAM-4 receptors

It is known that in mature RBCs, ICAM-4 is the major receptor for the endothelial integrin $\alpha v\beta 3$ (11,19). To show that our measurement technique is specific to $\alpha v\beta 3$, we first performed experiments on RBCs from healthy volunteers to obtain the baseline CF of active ICAM-4 receptors and unbinding forces between the $\alpha v\beta 3$ ligand and ICAM-4 receptor. Fig. 2 *A* (i) shows a representative force map recorded during the surface scan. There are 32×32 pixels in each force map. The color of the pixels indicates force values ranging between 0 and 100 pN according to the color scale shown in Fig. 2 *A*. We show that treatment of RBCs from healthy subjects with epinephrine, a catecholamine that binds to β2-ARs and activates the cAMP-PKA-dependent pathway, significantly increased the CF of active ICAM-4 receptors (Fig. 2 *C*) compared with baseline. When we first treated the sample with epinephrine and then with bath $\alpha v\beta 3$, we saw a dramatic decrease in the CF of detected unbinding events compared with the CF measured when the sample was incubated only with epinephrine (Fig. 2, *A* (iii) and *C*), suggesting that $\alpha v\beta 3$ in the bath blocked most of the active ICAM-4 receptors on the RBC membrane. In addition, we performed experiments with a cantilever treated with 3-aminopropyltriethoxysilane, glutaraldehyde, and BSA, but not with $\alpha v\beta 3$ (nonfunctionalized cantilever). The recorded CF was negligible (0.62%), meaning that $\alpha v\beta 3$ is indeed the functional protein on the cantilever tip (see Supporting Materials and Methods and Fig. S3). In addition, this measurement defined the background noise of the SMFS method for the specific assay described here.

Immunocytochemistry

For immunocytochemistry, 70 μL of normal or sickle blood was added to assigned wells containing poly-D-lysine-coated coverslips and incubated at 37°C for 15 min. After incubation, the wells were washed with Dulbecco's PBS (dPBS; ThermoFisher Scientific, Waltham, MA) and incubated with 16.39 nM of epinephrine (Sigma-Aldrich) or 1 μL of DI water carrier

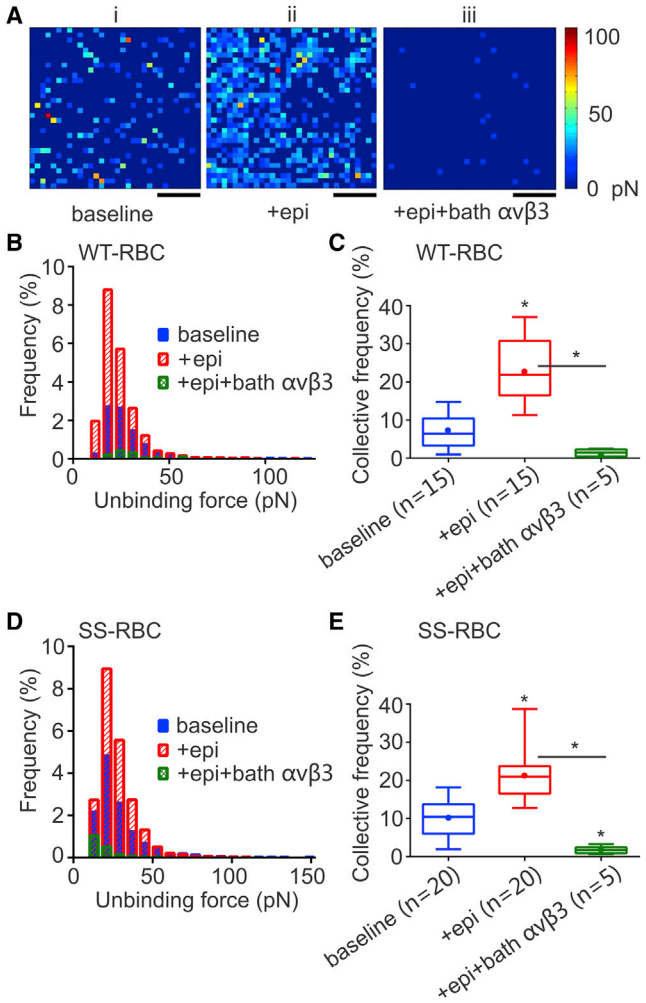

FIGURE 2 Distribution of active ICAM-4 receptors and unbinding force between $\alpha v\beta 3$ and ICAM-4. (*A*) Representative force maps from a 1 μm × 1 μm area of an individual RBC (i) at baseline, (ii) treated with 16.39 nM epinephrine, and (iii) treated with 16.39 nM epinephrine and 1.29 μg/mL bath $\alpha v\beta 3$ to block activated ICAM-4. Scale bars, 250 nm. The color scale indicates the magnitude of the unbinding force. (*B*) Frequency distributions of unbinding forces between ICAM-4 and $\alpha v\beta 3$ in WT-RBCs. (*C*) Box-and-whisker plot of the CF of active ICAM-4 receptors on WT-RBCs. Data are shown as the median with minimum and maximum whiskers, and the mean is denoted as a color dot. The *n* on the *x* axis indicates the total number of mature WT-RBCs analyzed in each group, obtained from the following numbers of human subjects: baseline: 3 subjects; + epinephrine: 3 subjects; + epinephrine + bath $\alpha v\beta 3$: 1 subject. Significance relative to baseline or between conditions, $^*p < 0.0001$. (*D*) Frequency distributions of unbinding forces between ICAM-4 and $\alpha v\beta 3$ in SS-RBCs. (*E*) Box-and-whisker plot of the CF of active ICAM-4 receptors on SS-RBCs. Data are shown as the median with minimum and maximum whiskers, and the mean is denoted as a color dot. The *n* on the *x* axis indicates the total number of mature SS-RBCs analyzed in each group, obtained from the following numbers of human subjects: baseline: 4 subjects; + epinephrine: 4 subjects; + epinephrine + bath $\alpha v\beta 3$: 1 subject. Significance relative to baseline or between two conditions, $^*p < 0.0001$. To see this figure in color, go online.

for 30 min at 37°C. Then, 1.29 μg/mL of human integrin $\alpha v\beta 3$ protein (Millipore) was added to all of the wells for 30 min at 37°C, followed by washing with dPBS. The cells were then fixed with 2% paraformaldehyde/4% sucrose/PBS for 5 min at room temperature. After washing with

dPBS and blocking with preblock buffer (20 mM phosphate buffer, pH 7.4, 5% normal goat serum, 450 mM NaCl) for 1 h at 4°C, the cells were incubated with mouse anti-integrin $\alpha v\beta 3$ primary antibody (1:500; catalog No. ab78289, Abcam, Cambridge, MA) in preblock buffer overnight at 4°C.

The next day, the cells were incubated with preblock buffer for 1 h at 4°C and then incubated with goat anti-mouse Alexa Fluor 488 secondary antibody (1:500; catalog No. ab150113, Abcam) in preblock buffer for 2 h in the dark. The cells were then washed with dPBS and coverslips were mounted on glass slides using ProLong Diamond mounting media (ThermoFisher Scientific, Waltham, MA).

Image acquisition

All images were taken on a laser-scanning Leica SP8 confocal microscope (Leica Microsystems, Wetzlar, Germany). Z-stacks were taken with a step size of 0.25 μm. For paraformaldehyde-fixed cells, a 63× oil immersion lens was used to view the cells, the pinhole size was set at 1 airy unit, and the raw images were exported as .tiff files and viewed on ImageJ software (National Institutes of Health, Bethesda, MD). For all acquired images, only the brightness and contrast for the entire frame were adjusted in ImageJ, and no singular section of the frame was modified in any way.

Image quantitation

Z-stacks from a cell were projected using the Z-project function of ImageJ software. To quantify the fluorescence intensity of the green (active ICAM-4) channel, a region of interest (ROI) was chosen and the measurement analysis was set to yield the area, minimum and maximum pixel strengths, integrated and raw densities, and mean grayscale value. The raw values were exported to Excel. The corrected total fluorescence (CTF) was calculated for the chosen ROIs for cells in the different conditions. The CTF is the resultant output of subtracting the mean background intensity over the chosen ROI from the integrated density for each ROI.

Statistical analysis

The unbinding forces between $\alpha v\beta 3$ ligands and ICAM-4 receptors are reported using the frequency (%) distribution, which states the percentage of events whose unbinding forces are within each bin's width. We then compare the median values of the forces measured in experiments without and with treatment with different reagents. The zero force points are not shown because they would obscure the plots since their population is much larger than the population of unbinding events. The CF% is related to the population of active ICAM-4 receptors and is defined as the percentage of all unbinding events divided by the total number of measurements, which is $32 \times 32 = 1024$ for each cell multiplied by the number of tested cells for each blood sample. The CF and CTF results are reported as the mean ± standard error (SE) and illustrated by box-and-whisker plots (GraphPad Prism, GraphPad Software, San Diego, CA). They are compared using one-way analysis of variance (ANOVA) and the Tukey-Kramer post hoc test. The results are considered significant if $p < 0.05$.

RESULTS AND DISCUSSION

Epinephrine increases the surface density of active ICAM-4 receptors on normal RBCs and SS-RBCs, but not the unbinding force between ICAM-4 and $\alpha v\beta 3$

Epinephrine is a hormone whose action is mediated by the β-AR, a seven-transmembrane domain receptor that can activate guanine nucleotide regulatory binding proteins (G protein-coupled receptors) (50). It was previously shown that activation of the cAMP-PKA-dependent pathway by epinephrine increases the adhesion of SS-RBCs, but not normal RBCs, to the endothelium via an ICAM4-$\alpha v\beta 3$ interaction (11). The experimental technique employed in that study was based on the flow-chamber assay, which measures the overall RBC adhesion and not directly the population of functional adhesion receptors or the strength of interactions between ligand-receptor pairs.

Here, we used the SMFS assay, which, as established in our previous work (12,13), can detect variations of the surface density of active adhesion receptors on the RBC membrane (i.e., CF%) and record unbinding forces between receptors and ligands. We scanned a 1 μm^2 area of individual RBC membranes with an AFM cantilever functionalized with $\alpha v\beta 3$ to directly detect the population of active ICAM-4 receptors under different experimental conditions. We first tested RBCs from healthy volunteers (WT-RBCs) at baseline and after in vitro treatment with epinephrine. The force maps shown in Fig. 2 *A* (i and ii) clearly illustrate that epinephrine increased the CF of active ICAM-4 receptors. However, epinephrine had no effect on the median unbinding force (Fig. 2 *B*; Table 2), suggesting that epinephrine affects only the activation of ICAM-4 receptors, and not the strength of their interaction with the $\alpha v\beta 3$ ligand.

To establish a measure of the overall quantity of active ICAM-4 receptors, we calculated the CF. The results are reported in box-and-whisker plots in Fig. 2 *C*. We found that the mean value of the CF increased significantly from 7.1% in baseline experiments to 23.63% when the blood sample was treated with epinephrine ($p < 0.0001$). This suggests that epinephrine triggers the activation of ICAM-4 receptors on WT-RBCs, probably via the cAMP-PKA pathway.

Next, we tested RBCs obtained from volunteers with SCD (SS-RBCs). We measured the CF of ICAM-4 receptors with and without treatment with epinephrine. Similar to the case with WT-RBCs, we found that the median unbinding force between ICAM-4 and $\alpha v\beta 3$ did not change

TABLE 2 Unbinding Forces and Collective Frequencies for WT-RBCs and SS-RBCs

	Unbinding Force (Median, pN)		Collective Frequency (Mean ± SE, %)	
	WT	SS	WT	SS
Test condition				
Baseline	24.59	23.59	7.10 ± 1.26	10.08 ± 0.85
+epi	24.27	24.53	23.63 ± 2.23	21.41 ± 2.27
+epi+bath $\alpha v\beta 3$	*	*	1.43 ± 0.37	1.78 ± 0.31
+FSK	24.08	24.70	25.91 ± 3.71	26.55 ± 2.68
+St-Ht31+FSK	27.45	26.09	7.80 ± 2.16	9.22 ± 1.52
+St-Ht31P+FSK		*		36.56 ± 8.73
+St-Ht31P	25.09	21.94	7.56 ± 1.81	10.12 ± 2.32

*There were not enough nonzero unbinding force data to generate an accurate median value.

significantly (Table 2; Fig. 2 *D*). The CF of ICAM-4 adhesion was measured to be 10.08% ± 0.85% for SS-RBCs without epinephrine treatment, which is higher than that found for WT-RBCs, but not significantly so ($p = 0.06$). Treatment of SS-RBCs with epinephrine increased the CF significantly to 21.41% ± 2.27% ($p < 0.0001$; Fig. 2 *E*; Table 2).

Our results are in agreement with previous experimental results showing that epinephrine increases adhesion of SS-RBCs to the endothelium (11). Moreover, our findings indicate that this increase is due to the increased number of active surface ICAM-4 molecules, and not to an increased unbinding force between ICAM-4 and $\alpha v\beta 3$. We note, however, that Zennadi et al. (11) did not detect a significant effect of epinephrine on WT-RBC adhesion to human umbilical vein endothelial cells. One possible reason for this discrepancy is that they incubated blood samples with 20 nM epinephrine for only 1 min at 37°C, whereas we incubated the samples with 16.39 nM epinephrine for 30 min at 37°C. Another possible explanation is that their method is not as sensitive to changes when the overall adhesion is low. They used intermittent flow conditions in a flow chamber and reported the ratio of the number of RBCs that adhered to human umbilical vein endothelial cells after exposure to flow conditions to the number of initially adherent RBCs before exposure to flow, whereas we directly measured the surface density of ICAM-4 at the single-molecule level. Cell-cell and cell-matrix adhesion may be influenced not only by the number of adhesion pairs between molecules expressed on the cells but also by the mechanical properties of cells (40,51). Our results, based on SMFS, provide direct evidence that the unbinding force between ICAM-4 and $\alpha v\beta 3$ did not change when the cells were incubated with epinephrine, meaning that ICAM-4 activation did not alter the interaction between ICAM-4 and $\alpha v\beta 3$, and did not cause the formation of nanoclusters. We note that these conclusions cannot be drawn using methods that directly measure RBC adhesion, such as microfluidics and single-cell force spectroscopy.

To validate the specificity of our measurements, we added $\alpha v\beta 3$ to the bath solution. We expected the bath $\alpha v\beta 3$ to bind to activated ICAM-4 receptors on the RBC membrane, thereby inhibiting cantilever-bound $\alpha v\beta 3$ from binding to ICAM-4 on the RBC surface. Indeed, binding significantly decreased in both WT-RBCs (CF 23.63% ± 2.23% vs. 1.43% ± 0.37%, $p < 0.0001$) and SS-RBCs (CF 21.41% ± 2.27% vs. 1.78% ± 0.31%, $p < 0.0001$; Fig. 2; Table 2). These results confirmed that indeed it is $\alpha v\beta 3$ that binds to the receptors on the RBC membrane, and not other substances attached to the cantilever, such as glutaraldehyde. Since our AFM cantilever functionalization technique involves the use of glutaraldehyde (52,53) to attach the $\alpha v\beta 3$ molecules to the cantilever, we wanted to test whether glutaraldehyde, with its inability to control the number of $\alpha v\beta 3$ molecules attached to the cantilever, would skew the results. To this end, we functionalized AFM cantilevers with $\alpha v\beta 3$ via an acetal-PEG-NHS linker instead of glutaraldehyde, which guarantees that the probability that the AFM cantilever will be functionalized with only one molecule is >50% (54) (Fig. 3, *A* and *B*). As demonstrated in Fig. 3, we probed SS-RBCs at baseline and found that both functionalization methods gave almost identical results with respect to the unbinding force (23.08 pN for the glutaraldehyde functionalization vs. 25.85 pN for the acetal-PEG-NHS functionalization, $p = 0.8451$) and CF (7.37% ± 1.45% for the glutaraldehyde functionalization vs. 8.44% ± 1.75% for the acetal-PEG-NHS functionalization, $p = 0.6943$; data not shown). This result means that ICAM-4 receptors expressed on the RBC membrane do not form nanoclusters, since the median values of the measured unbinding forces were similar for both techniques. If the receptors had formed nanoclusters, higher unbinding forces would have been recorded forming a second peak in the unbinding force histogram, as was the case in Abiraman et al. (38).

Confocal microscopy experiments confirm the SMFS-based results

We performed confocal microscopy experiments to image active ICAM-4 receptors on RBCs to further confirm our

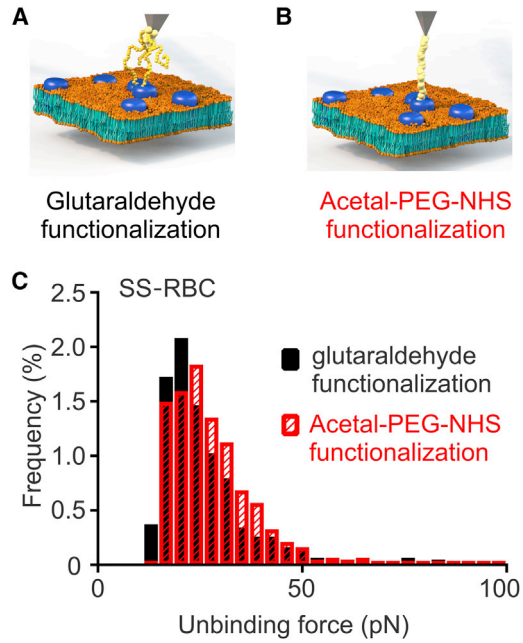

FIGURE 3 Comparison of ICAM4-$\alpha v\beta 3$ unbinding forces measured using glutaraldehyde-based versus PEG-based AFM cantilever functionalization. (*A*) Schematic of a glutaraldehyde-$\alpha v\beta 3$-functionalized tip probing ICAM-4 molecules on the RBC membrane. (*B*) Schematic of an acetal-PEG-NHS-$\alpha v\beta 3$-functionalized tip probing ICAM4 molecules on the RBC membrane. (*C*) Frequency distributions of unbinding forces between ICAM-4 and $\alpha v\beta 3$ on SS-RBCs for glutaraldehyde-based (*black*) and PEG-base (*red*) AFM cantilever functionalization. The same samples were used in both methods (two subjects, $n = 10$). To see this figure in color, go online.

SMFS-based findings. Both WT-RBCs and SS-RBCs were incubated with $\alpha v\beta 3$ (1.29μg/ml for 30 min) to tag active ICAM-4. The RBCs were then washed thoroughly to remove any unbound $\alpha v\beta 3$, fixed, and stained with anti-$\alpha v\beta 3$ antibody to label the $\alpha v\beta 3$ bound to the active ICAM-4. Alexa Fluor 488 was used to visualize active ICAM-4. Similar to the case with our AFM experiments, we found no significant difference in active ICAM-4-expression between WT-RBCs and SS-RBCs (Fig. 4, *A–C*, WT: CTF = 9.72 ± 0.63, $n = 16$; SS: CTF = 11.79 ± 0.47, $n = 16$; $p = 0.794$; Movies S1 and S2).

However, when WT-RBCs and SS-RBCs were incubated with epinephrine (16.39 nM for 30 min at 37°C) before being fixed and stained with anti-$\alpha v\beta 3$ antibody, we found a significant increase in active ICAM-4 expression compared with baseline in both cases (Fig. 4, *A–C*, WT: CTF = 16.29 ± 1.91, $n = 10$, $p = 0.033$; SS: CTF = 17.01 ± 0.92, $n = 16$, $p < 0.0001$). In addition to the confocal experiments, we performed AFM experiments on the same samples to compare the CF of unbinding events between WT- and SS-RBCs at baseline and when the cells were incubated with epinephrine. We found that there was no significant difference in the CF of unbinding events between WT- and SS-RBCs ($p > 0.5$), and addition of epinephrine caused a significant increase in the CF of unbinding events compared with baseline in both WT-RBCs ($p = 0.035$) and SS-RBCs ($p = 0.01$; Fig. S4). These results are in agreement with the results of the confocal microscopy experiments performed with the same samples, as well as with the overall AFM results discussed in the first section.

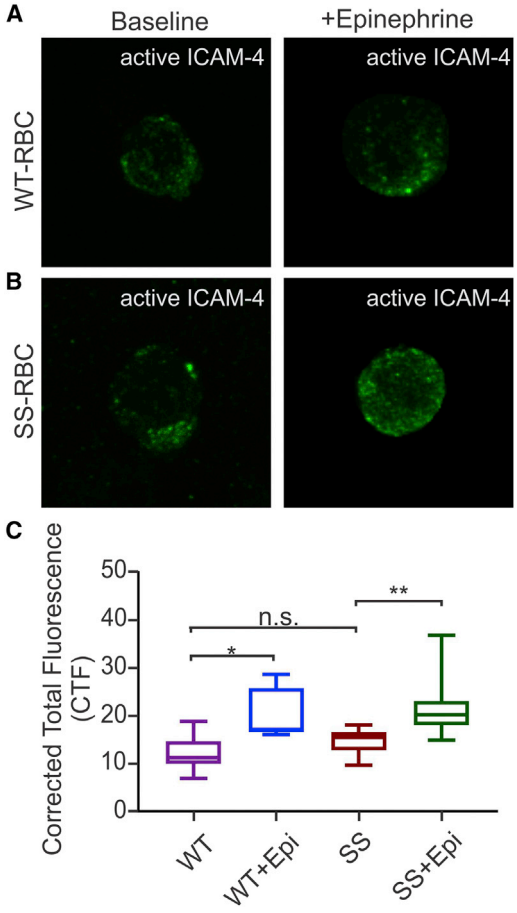

FIGURE 4 WT- and SS-RBCs were incubated with 16.39 nM of epinephrine or 1 μL of DI water carrier. They were then incubated with $\alpha v\beta 3$ to label active ICAM-4, fixed, and stained with anti-$\alpha v\beta 3$ antibody to label the $\alpha v\beta 3$ bound to active ICAM-4. (*A* and *B*) Representative confocal microscopy images of (*A*) WT-RBC ($n = 16$) and WT-RBC + epinephrine ($n = 10$), and (*B*) SS-RBC ($n = 16$) and SS-RBC + epinephrine ($n = 16$). (*C*) Box-and-whisker plots of the CTF of active ICAM-4 receptors on WT-RBCs and SS-RBCs with or without epinephrine treatment. The data are represented as mean ± SE, $*p = 0.0339$, $**p = 0.0042$, n.s., no significant difference (one-way ANOVA; one subject). To see this figure in color, go online.

Activation of ICAM-4 on WT-RBCs and SS-RBCs is regulated by the cAMP-PKA-dependent pathway

It is known that epinephrine binding of the β-AR activates the cAMP-PKA-dependent pathway. Furthermore, Zennadi et al. (11) demonstrated that SS-RBC adhesion is regulated by the same pathway. Using SMFS, we tested at the single-molecule level whether the increased CF of active ICAM-4 receptors on WT-RBCs and SS-RBCs is controlled by the cAMP-PKA pathway. We introduced pharmacologic regulation by using biomedical reagents that act along the cAMP-PKA pathway. We first pretreated WT-RBCs with FSK (0.49 μM), an AC activator that strongly activates PKA. Compared with baseline, FSK-treated WT-RBCs exhibited no difference in unbinding force (24.59 vs. 24.08 pN, $p = 0.26$; Fig. 5 *A*; Table 2) but a significantly higher CF (7.10% ± 1.26% vs. 25.91% ± 3.71%, $p < 0.0001$; Fig. 5 *B*; Table 2). In agreement with the results for WT-RBCs, we detected a similar unbinding force (23.59 vs. 24.70 pN, $p = 0.32$; Fig. 5 *C*; Table 2) and significantly increased CF in SS-RBCs preincubated with FSK (0.49 μM) compared with baseline (26.55% ± 2.68% vs. 10.08% ± 0.85%, $p < 0.0001$; Fig. 5 *D*; Table 2). This indicates that the CF of active ICAM-4 receptors on WT- and SS-RBCs is regulated by the cAMP-PKA-dependent pathway and that the strength of adhesive interactions is not affected. We also conclude that because the strength of unbinding forces did not change significantly, clustering of ICAM-4 receptors was unlikely.

ICAM-4 receptor activation is dependent on AKAPs

It is known that the action of PKA is localized to specific submembrane domains through PKA binding to AKAPs (21,29,30). Based on this, we investigated whether AKAPs

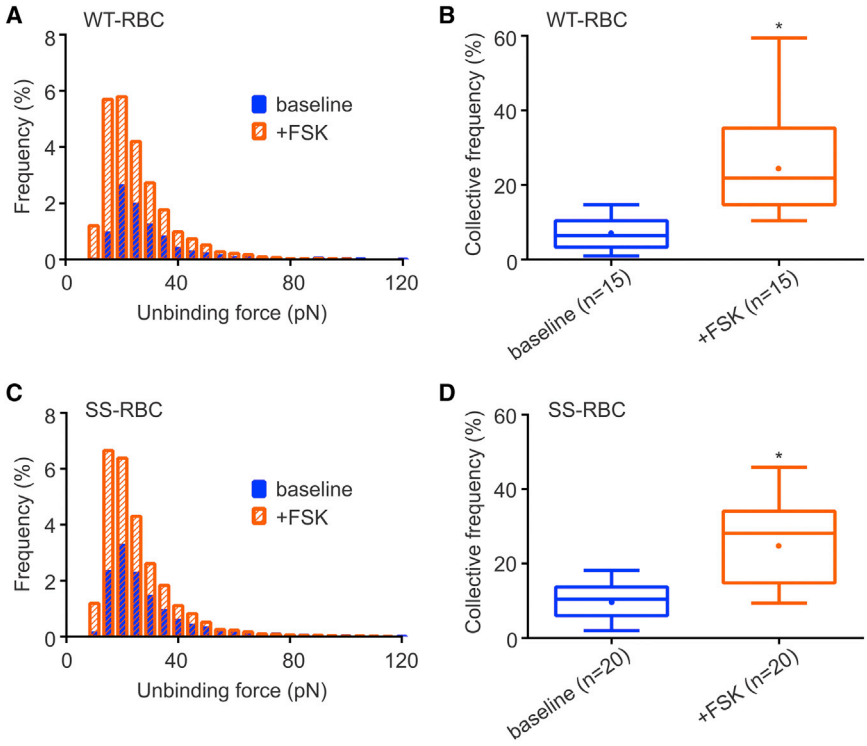

FIGURE 5 (*A*) Frequency distributions of unbinding forces between ICAM4 and $\alpha v\beta 3$ in WT-RBCs in the presence of the PKA activator FSK (0.49 μM). (*B*) Box-and-whisker plots showing the CF of active ICAM-4 receptors on WT-RBCs in the presence of FSK. Significance relative to baseline, $^*p < 0.0001$. The *n* on the *x* axis indicates the total number of WT-RBCs analyzed in each group: baseline: 3 subjects; FSK: 3 subjects. (*C*) Frequency distributions of unbinding forces between ICAM-4 and $\alpha v\beta 3$ in SS-RBCs in the presence of FSK (0.49 μM). (*D*) Box-and-whisker plots showing the CF of active ICAM-4 receptors on SS-RBCs in the presence of FSK. Significance relative to baseline, $^*p < 0.0001$. The *n* on the *x* axis indicates the total number of SS-RBCs analyzed in each group: baseline: 4 subjects; FSK: 4 subjects. To see this figure in color, go online.

located in the RBC membrane play a role in the PKA-dependent activation of ICAM-4 receptors. For this purpose, we used St-Ht31, a membrane-permeable peptide (55) comprising a PKA-anchoring domain that inhibits binding of PKA to AKAPs (56). As we discussed above, FSK activates AC, which in turn activates PKA and causes a significant increase in the CF of active ICAM-4 receptors on WT- and SS-RBCs. To demonstrate that ICAM-4 is activated via AKAPs, we incubated RBCs with St-Ht31 (2 h) and FSK (30 min) sequentially. In this case, the CF of active ICAM-4 on WT-RBCs was detected to be 7.80% ± 2.16%, in contrast to the 25.91% ± 3.71% obtained when only FSK was applied ($p < 0.0001$, Fig. 6 *A*; Table 2). Similarly, on SS-RBCs, CF was found to be 9.22% ± 1.52%, compared with 26.55 ± 2.68% when only FSK was applied ($p < 0.0001$, Fig. 6 *B*; Table 2). To confirm that the decrease was not due to a direct interaction between St-Ht31 and FSK, we pretreated SS-RBCs with St-Ht31P control peptide, which differs from St-Ht31 by isoleucine-to-proline substitutions and thus can no longer bind to PKA (56). We found that in this case the CF increased significantly (36.56% ± 8.73%, $p < 0.0001$; Table 2), demonstrating that indeed St-Ht31 inhibits activation of ICAM-4. When WT- and SS-RBCs were incubated solely with the control peptide St-Ht31P, the CF was similar to that of untreated samples (7.56% ± 1.81% for WT-RBCs and 10.12% ± 2.32% for SS-RBCs; Table 2). These results suggest that inhibition of the AKAP-PKA complex suppresses the activation of ICAM-4 receptors in both WT- and SS-RBCs.

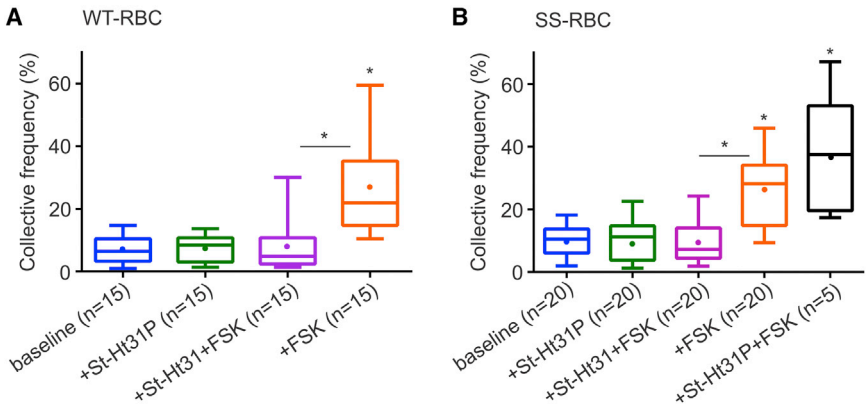

FIGURE 6 Modulation of active ICAM-4 via AKAPs on the RBC membrane. (*A* and *B*) Box-and-whisker plots of the CF of active ICAM-4 receptors on (*A*) WT-RBCs and (*B*) SS-RBCs for the reagents indicated on the *x* axis. The *n* on the *x* axis indicates the total number of mature RBCs analyzed in each group, obtained from the following numbers of human subjects: (i) for WT-RBCs, baseline: 3 subjects; St-Ht31P: 3 subjects; St-Ht31 (81.97 nM) + FSK (0.49 μM): 3 subjects. (ii) For SS-RBCs, baseline: 4 subjects; St-Ht31P: 4 subjects; St-Ht31 (81.97 nM) + FSK (0.49 μM): 4 subjects; St-Ht31P (81.97 nM) + FSK (0.49 μM): 1 subject. Significance relative to baseline or between conditions, $^*p < 0.0001$. To see this figure in color, go online.

CONCLUSIONS

In this study, we used SMFS and confocal microscopy to investigate at the single-molecule level the modulation of the surface density of active ICAM-4 receptors on WT- and SS-RBCs. Although it was known that epinephrine acts via the cAMP-PKA pathway to modulate the overall adhesion of SS-RBCs to endothelial cells, the mechanisms by which epinephrine acts at the single-molecule level were not known. Here, we demonstrated that epinephrine increases the surface expression of active ICAM-4 receptors in both WT- and SS-RBCs. Furthermore, we confirmed that the activation of ICAM-4 receptors is regulated via the cAMP-PKA pathway and, importantly, we determined for the first time, to our knowledge, that this activation is mediated by AKAPs. In addition, we showed that although the CF of active ICAM-4 receptors was modulated via the cAMP-PKA pathway, the median value of the unbinding force between active ICAM-4 and $\alpha v\beta 3$ did not change even at higher surface expressions of active ICAM-4. This means that activation of ICAM-4 did not alter the unbinding force between ICAM-4 and $\alpha v\beta 3$, and that nanoclusters of ICAM-4 were not formed in detectable numbers. This result, along with the finding that epinephrine activates ICAM-4 in both WT- and SS-RBCs, contrasts with results based on flow-chamber assays that showed that epinephrine did not significantly increase ICAM-4-dependent adhesion on WT-RBCs. Overall, our data might be of clinical importance in the context of drug development for the prevention and treatment of VOEs in SCD because they suggest that adhesion of RBCs to endothelial cells can be modulated, especially during stress conditions, by the introduction of biomedical reagents that act not only along the cAMP-PKA pathway but also on the AKAP-PKA complex.

SUPPORTING MATERIAL

Supporting Materials and Methods, four figures, and two movies are available at http://www.biophysj.org/biophysj/supplemental/S0006-3495(16)34273-4.

AUTHOR CONTRIBUTIONS

J.Z. designed experiments, performed AFM experiments and data analyses, and wrote the manuscript. K.A. designed experiments, performed confocal microscopy experiments and data analyses, and wrote the manuscript. S.-M.J. assisted with clinical protocol design and IRB regulatory requirements, enrolled volunteers, and collected blood specimens. G.L. designed experiments, performed data analyses, and wrote the manuscript. B.A. designed experiments, wrote the clinical protocol, recruited volunteers, oversaw IRB regulatory requirements, performed data analyses, and wrote the manuscript.

ACKNOWLEDGMENTS

We thank Kostyantyn Partola for preparing Fig. 3, *A* and *B*.

This work was supported by the Connecticut Institute for Clinical and Translational Science (CICATS) at the University of Connecticut. The content is the sole responsibility of the authors and does not necessarily represent the official views of CICATS. G.L. is supported by the National Science Foundation (CMMI-1235025, PHY-1205910) and the American Heart Association (12SDG12050688).

SUPPORTING CITATIONS

Reference (57) appears in the Supporting Material.

REFERENCES

1. Steinberg, M. H., and C. Brugnara. 2003. Pathophysiological-based approaches to treatment of sickle cell disease. *Annu. Rev. Med.* 54:89–112.
2. Rees, D. C., T. N. Williams, and M. T. Gladwin. 2010. Sickle-cell disease. *Lancet.* 376:2018–2031.
3. Ferrone, F. A. 2004. Polymerization and sickle cell disease: a molecular view. *Microcirculation.* 11:115–128.
4. Maciaszek, J. L., B. Andemariam, and G. Lykotrafitis. 2011. Microelasticity of red blood cells in sickle cell disease. *J. Strain Anal. Eng. Des.* 46:368–379.
5. Hillery, C. A., M. C. Du, …, J. P. Scott. 1996. Increased adhesion of erythrocytes to components of the extracellular matrix: isolation and characterization of a red blood cell lipid that binds thrombospondin and laminin. *Blood.* 87:4879–4886.
6. Hebbel, R. P., R. Osarogiagbon, and D. Kaul. 2004. The endothelial biology of sickle cell disease: inflammation and a chronic vasculopathy. *Microcirculation.* 11:129–151.
7. Zennadi, R., L. De Castro, …, M. J. Telen. 2008. Role and regulation of sickle red cell interactions with other cells: ICAM-4 and other adhesion receptors. *Transfus. Clin. Biol.* 15:23–28.
8. Du, E., M. Diez-Silva, …, S. Suresh. 2015. Kinetics of sickle cell biorheology and implications for painful vasoocclusive crisis. *Proc. Natl. Acad. Sci. USA.* 112:1422–1427.
9. Odièvre, M. H., E. Verger, …, J. Elion. 2011. Pathophysiological insights in sickle cell disease. *Indian J. Med. Res.* 134:532–537.
10. Hebbel, R. P., M. A. Boogaerts, …, M. H. Steinberg. 1980. Erythrocyte adherence to endothelium in sickle-cell anemia. A possible determinant of disease severity. *N. Engl. J. Med.* 302:992–995.
11. Zennadi, R., P. C. Hines, …, M. J. Telen. 2004. Epinephrine acts through erythroid signaling pathways to activate sickle cell adhesion to endothelium via LW-alphavbeta3 interactions. *Blood.* 104:3774–3781.
12. Maciaszek, J. L., B. Andemariam, …, G. Lykotrafitis. 2014. AKAP-dependent modulation of BCAM/Lu adhesion on normal and sickle cell disease RBCs revealed by force nanoscopy. *Biophys. J.* 106:1258–1267.
13. Maciaszek, J. L., B. Andemariam, …, G. Lykotrafitis. 2012. Epinephrine modulates BCAM/Lu and ICAM-4 expression on the sickle cell trait red blood cell membrane. *Biophys. J.* 102:1137–1143.
14. Hines, P. C., Q. Zen, …, L. V. Parise. 2003. Novel epinephrine and cyclic AMP-mediated activation of BCAM/Lu-dependent sickle (SS) RBC adhesion. *Blood.* 101:3281–3287.
15. Hebbel, R. P., O. Yamada, …, J. W. Eaton. 1980. Abnormal adherence of sickle erythrocytes to cultured vascular endothelium: possible mechanism for microvascular occlusion in sickle cell disease. *J. Clin. Invest.* 65:154–160.
16. Mohandas, N., and E. Evans. 1984. Adherence of sickle erythrocytes to vascular endothelial cells: requirement for both cell membrane changes and plasma factors. *Blood.* 64:282–287.
17. Grabowski, E. F. 1987. Sickle erythrocytes adhere to endothelial cell monolayers (ECM's) exposed to flowing blood. *Prog. Clin. Biol. Res.* 240:167–179.

18. Hoover, R., R. Rubin, …, R. Warren. 1979. Adhesion of normal and sickle erythrocytes to endothelial monolayer cultures. *Blood.* 54:872–876.
19. Telen, M. J. 2007. Role of adhesion molecules and vascular endothelium in the pathogenesis of sickle cell disease. *Hematology (Am. Soc. Hematol. Educ. Program).* 2007:84–90.
20. Telen, M. J. 2005. Erythrocyte adhesion receptors: blood group antigens and related molecules. *Transfus. Med. Rev.* 19:32–44.
21. Benovic, J. L. 2002. Novel β2-adrenergic receptor signaling pathways. *J. Allergy Clin. Immunol.* 110 (6, Suppl):S229–S235.
22. Eyler, C. E., T. Jackson, …, M. J. Telen. 2008. beta(2)-Adrenergic receptor and adenylate cyclase gene polymorphisms affect sickle red cell adhesion. *Br. J. Haematol.* 141:105–108.
23. Benovic, J. L., M. Bouvier, …, R. J. Lefkowitz. 1988. Regulation of adenylyl cyclase-coupled beta-adrenergic receptors. *Annu. Rev. Cell Biol.* 4:405–428.
24. Lefkowitz, R. J., B. K. Kobilka, …, M. G. Caron. 1988. Molecular biology of adrenergic receptors. *Cold Spring Harb. Symp. Quant. Biol.* 53:507–514.
25. Muravyov, A. V., V. B. Koshelev, …, S. V. Bulaeva. 2011. The role of red blood cell adenylyl cyclase activation in changes of erythrocyte membrane microrheological properties. *Biochem (Mosc.) Suppl. Ser. A Membr. Cell Biol.* 5:128–134.
26. Wong, W., and J. D. Scott. 2004. AKAP signalling complexes: focal points in space and time. *Nat. Rev. Mol. Cell Biol.* 5:959–970.
27. Tröger, J., M. C. Moutty, …, E. Klussmann. 2012. A-kinase anchoring proteins as potential drug targets. *Br. J. Pharmacol.* 166:420–433.
28. Taylor, S. S., J. A. Buechler, and W. Yonemoto. 1990. cAMP-dependent protein kinase: framework for a diverse family of regulatory enzymes. *Annu. Rev. Biochem.* 59:971–1005.
29. Murphy, B. J., and J. D. Scott. 1998. Functional anchoring of the cAMP-dependent protein kinase. *Trends Cardiovasc. Med.* 8:89–95.
30. Dell'Acqua, M. L., and J. D. Scott. 1997. Protein kinase A anchoring. *J. Biol. Chem.* 272:12881–12884.
31. Beene, D. L., and J. D. Scott. 2007. A-kinase anchoring proteins take shape. *Curr. Opin. Cell Biol.* 19:192–198.
32. Alessandrini, A., and P. Facci. 2005. AFM: a versatile tool in biophysics. *Meas. Sci. Technol.* 16:R65–R92.
33. Brown, A. E., R. I. Litvinov, …, J. W. Weisel. 2007. Forced unfolding of coiled-coils in fibrinogen by single-molecule AFM. *Biophys. J.* 92:L39–L41.
34. Müller, D. J., and Y. F. Dufrêne. 2011. Force nanoscopy of living cells. *Curr. Biol.* 21:R212–R216.
35. Maciaszek, J. L., H. Soh, …, G. Lykotrafitis. 2012. Topography of native SK channels revealed by force nanoscopy in living neurons. *J. Neurosci.* 32:11435–11440.
36. Müller, D. J., and Y. F. Dufrêne. 2011. Atomic force microscopy: a nanoscopic window on the cell surface. *Trends Cell Biol.* 21:461–469.
37. Lim, T. S., S. R. K. Vedula, …, C. T. Lim. 2008. Single-molecular-level study of claudin-1-mediated adhesion. *Langmuir.* 24:490–495.
38. Abiraman, K., M. Sah, …, A. V. Tzingounis. 2016. Tonic PKA activity regulates SK channel nanoclustering and somatodendritic distribution. *J. Mol. Biol.* 428:2521–2537.
39. Bartolucci, P., V. Chaar, …, W. El Nemer. 2010. Decreased sickle red blood cell adhesion to laminin by hydroxyurea is associated with inhibition of Lu/BCAM protein phosphorylation. *Blood.* 116:2152–2159.
40. Qian, J., and H. Gao. 2010. Soft matrices suppress cooperative behaviors among receptor-ligand bonds in cell adhesion. *PLoS One.* 5:e12342.
41. Davis, B. H., and N. C. Bigelow. 1994. Reticulocyte analysis and reticulocyte maturity index. *Methods Cell Biol.* 42:263–274.
42. Proksch, R., T. E. Schäffer, …, M. B. Viani. 2004. Finite optical spot size and position corrections in thermal spring constant calibration. *Nanotechnology.* 15:1344.
43. Walters, D. A., J. P. Cleveland, …, V. Elings. 1996. Short cantilevers for atomic force microscopy. *Rev. Sci. Instrum.* 67:3583–3590.
44. Maciaszek, J. L. 2013. Sickle cell disease erythrocyte stiffness and cytoadhesion investigated via atomic force microscopy. PhD dissertation, University of Connecticut, Storrs, CT. http://digitalcommons.uconn.edu/dissertations.
45. Partola, K. R., and G. Lykotrafitis. 2016. FRAME (force review automation environment): MATLAB-based AFM data processor. *J. Biomech.* 49:1221–1224.
46. Maciaszek, J. L., K. Partola, …, G. Lykotrafitis. 2014. Single-cell force spectroscopy as a technique to quantify human red blood cell adhesion to subendothelial laminin. *J. Biomech.* 47:3855–3861.
47. Tshiprut, Z., J. Klafter, and M. Urbakh. 2008. Single-molecule pulling experiments: when the stiffness of the pulling device matters. *Biophys. J.* 95:L42–L44.
48. Noy, A. 2011. Force spectroscopy 101: how to design, perform, and analyze an AFM-based single molecule force spectroscopy experiment. *Curr. Opin. Chem. Biol.* 15:710–718.
49. Noy, A., and R. W. Friddle. 2013. Practical single molecule force spectroscopy: how to determine fundamental thermodynamic parameters of intermolecular bonds with an atomic force microscope. *Methods.* 60:142–150.
50. Bylund, D. B. 2013. Adrenergic receptors. *In* Encyclopedia of Biological Chemistry, 2nd ed. W. J. Lennarz and M. D. Lane, editors. Elsevier, Amsterdam, The Netherlands, pp. 57–60.
51. Qian, J., J. Wang, and H. Gao. 2008. Lifetime and strength of adhesive molecular bond clusters between elastic media. *Langmuir.* 24:1262–1270.
52. Moy, V. T., Y. Jiao, …, T. Sano. 1999. Adhesion energy of receptor-mediated interaction measured by elastic deformation. *Biophys. J.* 76:1632–1638.
53. Zhang, X., S. E. Craig, …, V. T. Moy. 2004. Molecular basis for the dynamic strength of the integrin alpha4beta1/VCAM-1 interaction. *Biophys. J.* 87:3470–3478.
54. Wildling, L., B. Unterauer, …, H. J. Gruber. 2011. Linking of sensor molecules with amino groups to amino-functionalized AFM tips. *Bioconjug. Chem.* 22:1239–1248.
55. Ma, L., F. Dong, …, X. Zha. 2011. Ht31, a protein kinase A anchoring inhibitor, induces robust cholesterol efflux and reverses macrophage foam cell formation through ATP-binding cassette transporter A1. *J. Biol. Chem.* 286:3370–3378.
56. Carr, D. W., Z. E. Hausken, …, J. D. Scott. 1992. Association of the type II cAMP-dependent protein kinase with a human thyroid RII-anchoring protein. Cloning and characterization of the RII-binding domain. *J. Biol. Chem.* 267:13376–13382.
57. Lee, L. G., C. H. Chen, and L. A. Chiu. 1986. Thiazole orange: a new dye for reticulocyte analysis. *Cytometry.* 7:508–517.

Biophysical Journal, Volume *112*

Supplemental Information

Regulation of Active ICAM-4 on Normal and Sickle Cell Disease RBCs via AKAPs Is Revealed by AFM

Jing Zhang, Krithika Abiraman, Sasia-Marie Jones, George Lykotrafitis, and Biree Andemariam

S1. cAMP-PKA dependent pathway and AKAPs

One important mechanism of ICAM-4 activation is via the cyclic adenosine monophosphate-protein kinase A (cAMP-PKA) dependent signaling pathway (Fig. S1) which can be mediated by A-kinase anchoring proteins (AKAPs). Activation of RBC β2-adrenergic receptors (β2-ARs), induced by epinephrine, activates the α subunit of the associated G protein (Gαs) by exchanging its bound guanosine diphosphate (GDP) to guanosine triphosphate (GTP). The activated Gαs, together with GTP, then dissociates from the β and γ subunit to further stimulate adenylyl cyclase (AC). AC (which can be directly activated, e.g. by forskolin) catalyzes the conversion of adenosine triphosphate (ATP) to cAMP which then activates PKA. A kinase anchoring protein (AKAPs) anchors PKA to specific sites on the plasma membrane where PKA can alter the phosphorylation state of neighboring ICAM-4 receptors thereby causing their activation. (See (1-3).

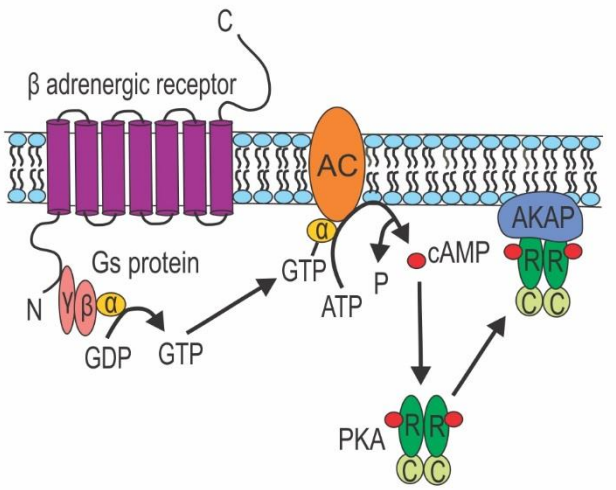

Figure S1. RBC cAMP-PKA dependent pathway.

S2. Reticulocytes

Thiazole orange has been proved to be an ideal fluorescent dye for reticulocyte analysis due to its good quantum yield, enhancement of fluorescence with RNA, membrane permeability, simple staining procedure and ability to count as many reticulocytes as new methylene blue and was therefore used to identify reticulocytes in the petri dish containing blood sample (4). The following protocol was employed: (1) Stock solution of 1 mg/mL Thiazole orange (purchased from Sigma-Aldrich, St. Louis, MO) in methanol was made. (2) The stock solution was diluted to 3×10^{-7} M in phosphate-buffered saline. (3) RBCs were seeded on a glass bottom petri dish, as we do for adhesion measurements, then 1mL 3×10^{-7} M Thiazole orange solution was added and incubated at room temperature for 1h. (4) Cells were then observed under fluorescence microscopy to identify reticulocytes (Fig. S2 A, B). As for the unstained control (Fig. S2 C, D), we followed the same protocol as described above but added PBS instead of Thiazole orange solution in step (3).

The reticulocyte count of the tested sample was 11.3%. Figure S2 A and B are representative bright-field and fluorescent microscopy images respectively of Thiazole orange stained RBCs. They show a representative area which contained both reticulocytes (in colored circles) which were excluded from our measurement and biconcave RBCs which were tested (in green triangles) to detect unbinding events. Figure S2 C and D are representative bright-field and fluorescent microscopy images respectively of unstained RBCs. As expected we did not observe any fluorescence.

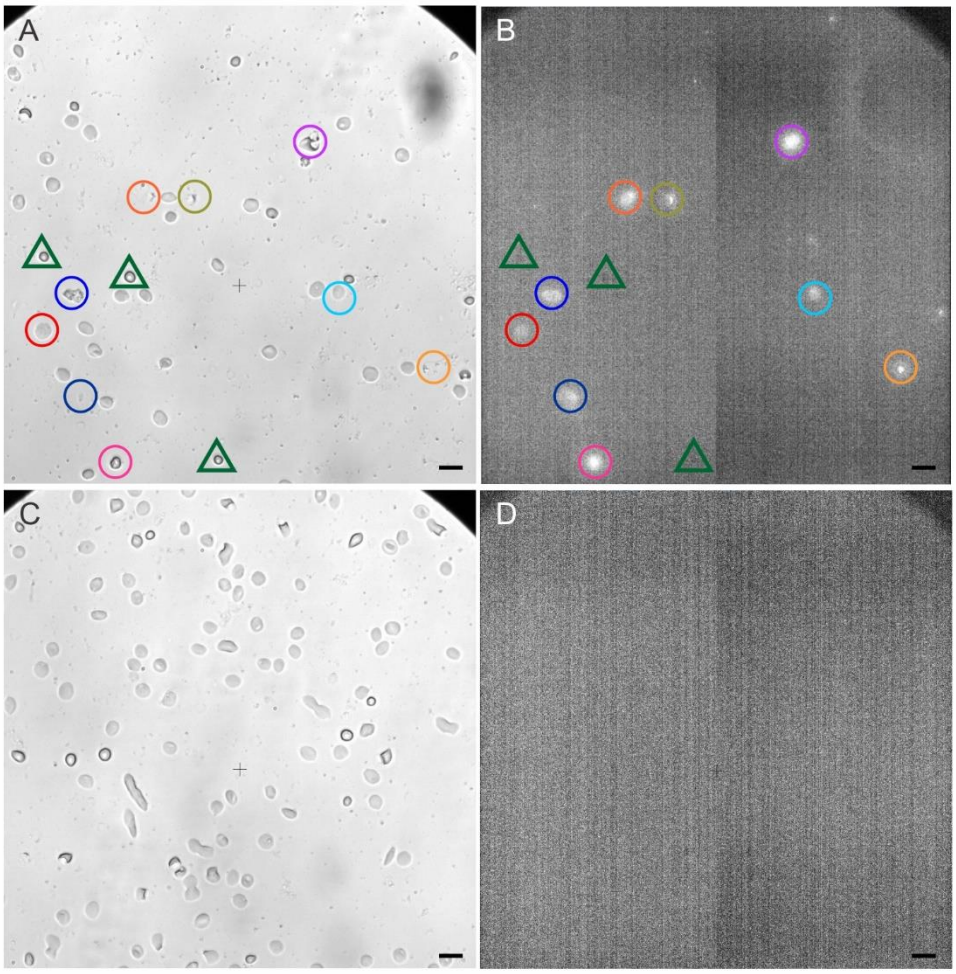

Figure S2. (A) Optical microscopy image of RBCs in Thiazole orange solution (B) Fluorescent microscopy image of RBCs in Thiazole orange solution. (C) Optical microscopy image of RBCs in PBS. (D) Fluorescent microscopy image of RBCs in PBS. The scale bar corresponds to 20μm.

S3. Results from the control experiments related to BSA coating of the probe

Here, we compare the histograms of unbinding forces and CF box-whisker plots of unbinding events between SS-RBCs and a probe coated with αvβ3 and then with BSA versus a cantilever coated only with BSA. We found a negligible number of unbinding events for non-αvβ3 coated probes.

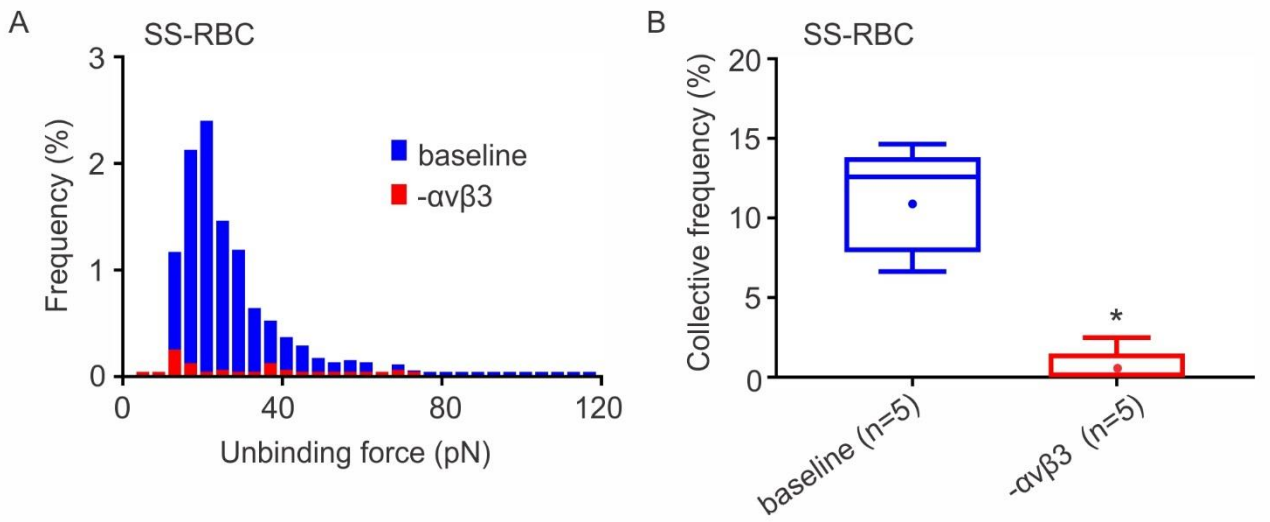

Figure S3. (A) Frequency distributions of unbinding forces between ICAM4 and αvβ3 in SS-RBCs for probes coated with αvβ3 and then BSA and for probes coated only with BSA and not with αvβ3. (B) Box-whisker plots showing the CF of active ICAM-4 receptors on SS-RBCs from probes coated with αvβ3 and then BSA and for probes coated only with BSA and not with αvβ3 (p=0.0001).

S4. Confocal microscopy experiments

Movie S1. Z stack of WT-RBCs labeled with αvβ3 antibody which tags the αvβ3 bound to active ICAM-4 receptor and imaged with laser-scanning Leica SP8 (Leica Microsystems, Wetzlar, Germany) confocal microscope.

Movie S2. Z stack of SS-RBCs labeled with αvβ3 antibody which tags the αvβ3 bound to active ICAM-4 receptor and imaged with laser-scanning Leica SP8 (Leica Microsystems, Wetzlar, Germany) confocal microscope.

S5. AFM experiments on the same samples as the confocal microscopy experiments

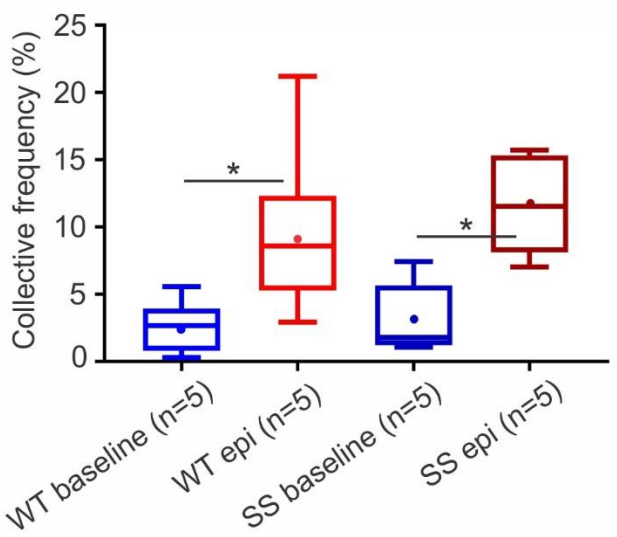

Figure S4. CF of the unbinding events at baseline and after treatment with epinephrine for the samples that were used in the confocal experiments shown in Figure 4. We found no significant difference in CF between WT- and SS-RBCs at the baseline and between WT and SS-RBCs after treatment with epinephrine. We found significant difference in CF between WT-RBCs at baseline and after treatment with epinephrine and between SS-RBCs at baseline and after treatment with epinephrine. The results are in agreement with the results from the confocal experiments performed on the same samples. (* signifies $p < 0.04$).

SUPPORTING REFERENCES

1. Lefkowitz, R. J., B. K. Kobilka, J. L. Benovic, M. Bouvier, S. Cotecchia, W. P. Hausdorff, H. G. Dohlman, J. W. Regan, and M. G. Caron. 1988. Molecular biology of adrenergic receptors. Cold Spring Harb Symp Quant Biol 53 Pt 1:507-514.
2. Benovic, J. L., M. Bouvier, M. G. Caron, and R. J. Lefkowitz. 1988. Regulation of adenylyl cyclase-coupled beta-adrenergic receptors. Annu Rev Cell Biol 4:405-428.
3. Wong, W., and J. D. Scott. 2004. AKAP signalling complexes: focal points in space and time. Nat Rev Mol Cell Bio 5:959-970.
4. Lee, L. G., C. H. Chen, and L. A. Chiu. 1986. Thiazole orange: a new dye for reticulocyte analysis. Cytometry 7:508-517.